International Tables for Crystallography (2013). Vol. D, Section 3.3.11, pp. 469–477.

tible and, hence, is designated here as *coherent*, even if the contact plane does not coincide with the twin mirror plane.

(iv) For non-merohedral (ferroelastic) twins, a pair of (rational or irrational) perpendicular compatible interfaces occurs (Section 3.3.10.2.1). The same holds for merohedral twins of lattice index $[j] > 1$ (Section 3.3.10.2.4). All these compatible boundaries are considered here as *coherent*.

(v) In lattice and structural terms, a twin boundary is *coherent* if it exhibits a well defined matching of the two lattices along the entire boundary, *i.e.* continuity with respect to their lattice vectors and lattice planes. We want to stress that we consider the coherence of a twin boundary not as being destroyed by the presence of a nonzero twin displacement or fault vector as long as there is an optimal low-energy fit of the two partner structures. The twin displacement (fault) vector represents a 'phase shift' between the two structures with the same two-dimensional periodicity along their contact plane and thus defines the continuity relation across the boundary. This statement agrees with the general opinion that stacking faults, antiphase boundaries and many merohedral twin boundaries, all possessing nonzero fault vectors, are *coherent*. Well known examples are stacking faults in f.c.c and h.c.p metals and Brazil twin boundaries in quartz.

It is apparent from these discussions of *coherent* twin interfaces that several features have to be taken into account, some readily available by experiments and observations, whereas others require geometric models (lattice matching) or even physical models (structure matching), including determination of twin displacement vectors **t**.

The definitions of *coherence*, as treated here, often do not satisfactorily agree with reality. Two examples are given:

(*a*) Japanese twins of quartz with twin mirror plane $(11\bar{2}2)$ or twofold twin axis normal to $(11\bar{2}2)$. According to the definitions given above, the observed $(11\bar{2}2)$ contact plane is *coherent*. Nevertheless, these $(11\bar{2}2)$ boundaries are always strongly disturbed and accompanied by extended lattice distortions. Thus, in reality they must be considered as *not coherent*.

(*b*) Sodium lithium sulfate, $NaLiSO_4$, with polar point group $3m$ and a hexagonal lattice forms merohedral growth twins with twin mirror plane (0001) normal to the polar axis. The composition plane coincides with the twin plane and has head-to-head or tail-to-tail character. According to definition (iii) above, any twin boundary of this merohedral twin is *coherent*. The observed (0001) contact plane, however, despite coincidence with the twin mirror plane, is always strongly disturbed and cannot be considered as coherent. In this case, the observed *incoherence* is obviously due to the head-to-head orientation of the boundary, which is 'electrically forbidden'.

These examples demonstrate that the above formal definitions of *coherence*, based on geometrical viewpoints alone, are not always satisfactory and require consideration of individual cases.

With these discussions of rather subtle features of twin interfaces, this part on twinning in direct space is concluded. It was our aim to present this rather ancient topic in a way that progresses from classical concepts to modern considerations, from three dimensions to two and from macroscopic geometrical arguments to microscopic atomistic reasoning. Macroscopic derivations of orientation and contact relations of the twin partners (twin laws, as well as twin morphologies and twin genesis) were followed by lattice considerations and structural implications of twinning. Finally, the physical background of twinning was explored by means of the analysis of twin interfaces, their structural and energetic features. It is this latter aspect which in the future is most likely to bring the greatest progress toward the two main goals, an atomistic understanding of the phenomenon 'twinning' and the ability to predict correctly its occurrence and non-occurrence.

3.3.11. Effect of twinning in reciprocal space

In the previous sections of this chapter the twinning phenomena were considered in *direct space*, in particular the orientation relations of the twin components (twin domains), *i.e.* the twin laws, and the contact relations, *i.e.* the interfaces between twin partners (twin boundaries). The present section extends these considerations to *reciprocal space*, *i.e.* to X-ray, neutron and electron diffraction of simple and multiple twins, including structure determinations on twinned crystals.

It should be emphasized that for these investigations only 'single-crystal' methods are applicable. Powder diffraction is *not* capable of revealing an existing twin, but is very useful for characterizing a crystal aggregate independent of twinning. In particular, powder patterns can reveal high-to-low-symmetry phase transitions, *e.g.* by splitting of diffraction peaks, which are the prerequisites of transformation twins and domain structures (*cf.* Section 3.3.7.2 and Chapter 3.4).

In many cases twins are difficult to detect. Methods for identifying twins and their twin laws in direct space (morphology, optics, X-ray topography *etc.*) are given in Section 3.3.6.1. Tests for twinning in the diffraction records, particularly statistical tests, and 'warning signs' of twinning are contained in Sections 7.5–7.7 of Herbst-Irmer (2006) and in the publication by Kahlenberg (1999).

3.3.11.1. *Basic features of twin diffraction records*

In the following, the basic features of the diffraction patterns of twins are summarized. They hold for any type of twin and even for intergrowths with any orientation relation, *e.g.* bicrystals or irregular grain assemblies.

(i) Whereas in direct space the various twin components are spatially separated, in reciprocal space all their diffraction records are superimposed with a common origin.

(ii) The orientation relations of the twin-related diffraction patterns in reciprocal space and of the corresponding domains in real space ('twin laws') are the same.

(iii) For a multiple twin with n orientation states [*cf.* Fig. 3.3.3.1(*c*)] all individual diffraction patterns are superimposed, whereby all twin components of the same orientation state contribute to the same diffraction pattern [*e.g.* polysynthetic twins, *cf.* Figs. 3.3.3.1(*b*) and 3.3.6.13].

(iv) The diffraction pattern of a twin is – apart from the intensities of reflections – independent of the size, distribution and shape of the twin domains, as well as of their boundaries (contact relations). The intensities are governed by the volume fractions of the orientation states.

(v) Friedel's rule also applies to twins, *i.e.* the diffraction record of a twinned crystal is centrosymmetric, provided anomalous scattering is negligible. This implies that 'inversion twins' can only be detected by diffraction experiments if anomalous scattering is sufficiently high.

(vi) Since the twin partners are 'macroscopic' individuals (*cf.* the definition of twin in Section 3.3.2.1), the superposition of two or more twin-related diffraction patterns involves the addition of intensities, not of structure factors, as would be the case in superstructures, in so-called 'cell twinning' (*cf.* Takeuchi, 1997), or in 'modular' crystal structures [*cf.* Ferraris (2004) and Note (1) in Section 3.3.2.4].

Classification of twinning in reciprocal space. Whereas in direct space the twin elements and the morphological features are the main criteria of twin classification (*cf.* Sections 3.3.3 and 3.3.4), in reciprocal space the degree of overlapping of the various diffraction patterns is the dominant criterion and leads to the following subdivisions:

(*a*) General (non-merohedral, inclined-lattice) twins: no general overlap of the twin-related diffraction patterns, hence 'split reflections'; Section 3.3.11.2.

(*b*) Twins by (strict) merohedry (parallel-lattice $\Sigma 1$ twins): *complete* and *exact* overlap (coincidence) of the individual twin-related diffraction patterns, no 'split reflections'; Section 3.3.11.3.

(*c*) Twins by reticular merohedry (partially parallel-lattice twins, $\Sigma > 1$ twins): *exact* but *partial* overlap of twin-related diffraction patterns, no 'split reflections' but also 'single reflections'; Section 3.3.11.4.

(*d*) Twins by pseudo(-reticular) merohedry (pseudo-parallel-lattice twins): *approximate* complete or partial overlap of the twin-related diffraction patterns. Special problem: partially overlapped (partially split) reflections; Section 3.3.11.5.

3.3.11.2. *General (non-merohedral, inclined-lattice) twins*

This case refers to the most general type of twin, where the lattices of the two twin partners have one of the two minimal elements in common which are required by the definition of a 'crystallographic orientation relation' in Section 3.3.2.2(*a*):

(i) at least *one* lattice row (crystal edge) [*uvw*] *common* to both partners I and II, either parallel or antiparallel;

(ii) at least two lattice planes (crystal faces) $(hkl)_{\rm I}$ and $\pm(hkl)_{\rm II}$, one from each partner, *parallel*.

For the diffraction record this has the following consequences:

(i) If the common lattice row is a (rational) twofold twin axis [*uvw*] (binary twin), all lattice planes (*hkl*) belonging to the zone [*uvw*] are mapped upon themselves by the twin operation. They fulfil the zone condition $uh + vk + wl = 0$. In reciprocal space these planes form a single reciprocal plane (*hkl*) normal to the twofold twin axis in direct space. In the diffraction pattern of the twin this (zero-layer) reciprocal plane is common (coincident) to the diffraction patterns of the two twin components [for an illustration see Massa (2004), Fig. 11.7].

If the common lattice row is not a rational twofold twin axis, *e.g.* as in the case of twinning by the *Kantennormalengesetz* (complex twin, *irrational* twofold twin axis, *cf.* Fig. 3.3.2.3), reciprocal-lattice points (diffraction spots) common to the two individual diffraction patterns do not occur. This underlines the limiting character of this intergrowth as a kind of twinning.

(ii) If the common lattice plane is a twin reflection plane (*hkl*), this plane is mapped upon itself by the twin operation, and so is the perpendicular reciprocal lattice row *nh*, *nk*, *nl* (representing all orders of the reflection *hkl*). If the common lattice plane (*hkl*) results from an – in general irrational – twofold twin axis normal to it, exactly the same reciprocal row *nh*, *nk*, *nl* is common to the diffraction records of both twin individuals. This is due to the centrosymmetry of the direct and the reciprocal lattices, which leads to the equivalence of the twin mirror plane (*hkl*) and the twofold twin axis normal to it.

For the twinning by the *Kantennormalengesetz* with *irrational* twin reflection plane (*cf.* Fig. 3.3.2.3) there are again no diffraction spots (reciprocal-lattice points) common to the two individual diffraction patterns.

It is possible that other layer lines of the twin diffraction record also show coincidence features, due to metrical 'accidents' in the lattice constants of the crystal [illustration: Massa (2004), Fig. 11.8]. In general, however, the large number of non-overlapped reflections permits easy determination of the twin law, as well as determination of the volume ratio of the twins (comparison of the intensities of pairs of non-overlapped symmetry-equivalent reflections $hkl_{\rm I}$ and $hkl_{\rm II}$). Also, the structure determination is usually unproblematic since it can be done with the standard methods using the many non-overlapped reflections of the twin partner with the larger volume. If needed, even the overlapped reflections can be split into the two twin partners with the help of the previously determined volume fraction. Most twins belong to this type of 'general twins'.

For their investigation it is highly advisable to use two-dimensional Weissenberg or precession films or a two-dimensional detector which shows the splitting of the twin reflections in the reciprocal-lattice plane.

Note that actual twins may have – in addition to the minimum requirements given above – accidental reflection coincidences which depend on the twin law, the *eigensymmetry* and the metric of the crystal under consideration, as shown in the following examples.

Examples:

(i) *Dovetail twins of gypsum*, *eigensymmetry* $2_y/m_y$, twin reflection plane (100), *cf.* Section 3.3.4.1 and Fig. 3.3.4.1. Here the reciprocal-lattice row [*h*00] is common to both diffraction patterns. Moreover, since the twin operation also maps the lattice plane (010) upon itself, the reciprocal row [0*k*0] is also common to both patterns, *i.e.* both rows exhibit coincidence of the reflections of both partners. All other reflections are 'split reflections'.

(ii) A similar coincidence behaviour occurs for the frequent (110) *reflection twins of orthorhombic crystals* (*cf.* Fig. 3.3.4.2, twin domains 1 and 2). They map the direct-lattice planes (110) and (001) upon themselves, and thus the reciprocal-lattice rows *hh*0 and 00*l* are common to both diffraction patterns, with coinciding reflections.

(iii) A particularly illustrative example with both types of overlapping reflections are the triclinic plagioclase feldspars, with two famous twin laws (*cf.* Section 3.3.6.12):

Albite law: rational twin reflection plane (010); hence, the reflections of the (one-dimensional) reciprocal row [0*k*0] of both twin partners are superimposed in the twin diffraction record.

Pericline law: rational twofold twin rotation axis [010]; the lattice planes (*h*0*l*) belong to this zone. Hence, the reflections of the two-dimensional reciprocal layer *h*0*l* of both twin partners are superimposed in the diffraction set.

Descriptions of structure determinations (with diagrams) on general (non-merohedral) twins are contained in the following publications: Herbst-Irmer (2006, Sections 7.8.5 and 7.8.6), Massa (2004, Chapter 11), Dunitz (1964, pseudo-orthorhombic monoclinic twins) and Herbstein (1965, molecular crystal with albite twin law); many further examples exist in the literature.

3.3.11.3. *Twinning by (strict) merohedry (parallel-lattice twins, $\Sigma 1$ merohedral twins)*

In *direct space*, $\Sigma 1$ twins by merohedry (*cf.* Sections 3.3.8.2 and 3.3.9) are characterized by exact parallelism of the lattices of all twin domains, *i.e.* the coincidence-site lattice (CSL) or twin lattice is identical with the lattice of the untwinned crystal. The twin element, on the other hand, is a symmetry element of the point group of the lattice (holohedry) but not of the crystal, *i.e.* the (merohedral) crystal point group is a proper subgroup of its holohedry. This implies that only binary twin elements are possible: inversion, twofold rotation or reflection twins of index [2]. There are in total 63 possible merohedral twin laws in the 35 structural settings of the 26 merohedral crystal classes. They are completely listed and characterized in Appendices A and D (Tables 7–9) of Klapper & Hahn (2010). Note the large number of twin laws in the hexagonal crystal family.[8]

In *reciprocal space* the counterpart to lattice parallelism, described above, is the complete and exact superposition, with a common origin, of the diffraction patterns of all twin domains, *i.e.* each reflection in the diffraction record of the twin is the superposition of the twin-related intensities of all twin-domain states, according to their volume fraction.

For diffraction experiments and structure determinations on merohedral $\Sigma 1$ twins the above relations have the following consequences:

[8] A different listing of the merohedral twin laws is provided by Table 3.4.3.5 in Chapter 3.4 of this volume. It refers to macroscopic (tensor) properties; hence only group–subgroup relations (43 twin laws) are considered.

(i) Because of the complete overlap of the diffraction patterns and the parallelism of the symmetry elements, twinning by merohedry cannot be identified by diffraction experiments. In many cases structure refinements of merohedrally twinned crystals can simulate disorder. Hence, chemically or physically 'strange' disorder can be a hint for twinning, as are refinements with unusually large R values.

(ii) There are no 'strange' space-group extinctions as a clue to (strict) merohedral twinning, except for the following four cases:

(*a*) In space group $P2_1/a\bar{3}$ (No. 205), merohedral twinning causes 'violations' of the extinctions in the $\{0kl\}$ reflection sets, *cf.* Klapper & Hahn (2012), p. 83. Note that this 'violation' occurs for *all volume ratios* of the twins.

(*b*) In contrast, *only* for volume ratios exact or close to 1:1 (*i.e.* by simulation of the higher Laue class), the extinction rules of the following three space groups do not exist in the higher-symmetry Laue class: $P4_2/n$ (86), $I4_1/a$ (88) and $I2_1/a\bar{3}$ (206) [*cf. IT* A, Part 3, Table 3.1.4.1 and Massa (2004), p. 154]. These four cases are strong clues for twins by merohedry.

(iii) A strong indication for merohedral twinning can often be obtained if in several specimens of the crystal under investigation some groups of reflections vary in intensity whereas other stay constant. This is due to the three 'twin diffraction cases' A, B1 and B2, which differ in the way their twin-related reflection sets are 'affected' by the given twin law.

Case A: the twin-related reflection sets (face forms) are symmetry equivalent, *i.e.* their superimposed intensities are not affected by the twinning;

Case B2: the twin-related face forms are 'opposites' $\{hkl\}$ and $\{\bar{h}\bar{k}\bar{l}\}$, *i.e.* they differ only in their anomalous-scattering contributions, usually small;

Case B1: the twin-related reflections sets are neither symmetry equivalent nor opposite, *i.e.* their intensities are (often quite strongly) different and their superposition varies with the volume ratio. B1 reflection sets will vary from one specimen to the next, whereas the intensities of A and (in many cases) B2 reflections are relatively unchanged. This opens the possibility of attempting a structure determination only with A and B2 (if anomalous scattering is small) reflection sets. A detailed description of these reflection sets (face forms) and their use, with examples, is presented by Klapper & Hahn (2010). Their Table 9 lists the three 'twin diffraction cases' A, B1 and B2 for the seven reflection sets of all 63 $\Sigma1$ merohedral twin laws.

(iv) There is another useful subdivision of merohedral twins: Types I and II by Catti & Ferraris (1976).

Type I twins: the twin element belongs to the Laue symmetry of a noncentrosymmetric crystal (but, of course, *not* to its *eigensymmetry* point group). These twins can always be described as inversion twins, since the inversion is always part of their twin coset. Note that triclinic, monoclinic and orthorhombic crystals can only form merohedral type I twins, because these crystal systems have only one Laue class, whereas the higher-symmetry systems have two Laue classes. For structure determinations type I twins present no problems because, according to Friedel's rule, every diffraction record is centrosymmetric (neglecting anomalous scattering). Determinations of the 'absolute structure' and the 'absolute polarity' (*cf.* Klapper & Hahn, 2010), however, are not possible because inversion twins exhibit superposition of 'opposite' reflection sets (case B2 sets). Comparison of the measured and calculated (for an untwinned crystal) anomalous-scattering contributions often permits determination of the 'Flack factor' (Flack, 1983) and, hence, of the volume ratio of the two enantiomorphic or antipolar twin states. Type I merohedral twins can occur in any of the 21 noncentrosymmetric point groups (28 possible twin laws, *cf.* Table 9 in Klapper & Hahn, 2010).

Type II twins: These twins can only occur in all (centrosymmetric and noncentrosymmetric) point groups of the *lower-symmetry* Laue classes of the tetragonal ($4/m$), hexagonal ($\bar{3}$, $\bar{3}2/m$, $6/m$) and cubic ($2/m\bar{3}$) crystal family (13 point groups, 35 possible twin laws). Here the twin element is a symmetry element of the *higher-symmetry* Laue class ($4/mmm$, $\bar{3}2/m$,[9] $6/mmm$, $m\bar{3}m$), thus producing superposition of non-equivalent face forms, *i.e.* diffraction case B1, with volume-fraction dependent intensities, even for negligible anomalous scattering. If these intensities are used for structure refinement, disorder or possibly a hypothetical new modification is simulated. For volume fractions near 1:1 a higher-symmetry space group can even be found [for exceptions see topic (ii) above]. The best procedure – apart from finding an untwinned crystal – is to use refinement programs which include the refinement of the twin volume ratio.

(v) A special, interesting case exists for some naturally occurring amino acids, proteins, nucleic acids and related molecules. They are chiral and occur only with one handedness, *i.e.* these molecules are 'enantiomerically pure'. As a consequence crystals of these molecules are 'enantiomorphically pure' and occur with one handedness only. These crystals can, of course, occur only in one of the 11 enantiomorphic crystal classes and their twin laws can only be rotation twins. This combination, however, restricts the occurrence of merohedral $\Sigma1$ twins of these crystals still further: merohedral $\Sigma1$ *rotation* twins can only occur in tetragonal, trigonal, hexagonal and cubic crystals with the following seven point groups and structural settings (P = hexagonal P lattice, R = rhombohedral R lattice):

$$3\ (P),\ \ 321\ (P),\ \ 312\ (P),\ \ 3\ (R),\ \ 4,\ \ 6 \text{ and } 23.$$

The resulting number of $\Sigma1$ twin laws is reduced from 63 (*cf.* Table 9 in Klapper & Hahn, 2010) to nine:

$$\begin{aligned}&3(P) \rightarrow 321(P),\ \ 3(P) \rightarrow 312(P),\ \ 3(P) \rightarrow 6(P),\\&3(R) \rightarrow 32(R),\ \ 321(P) \rightarrow 622(P),\ \ 312(P) \rightarrow 622(P),\\&4 \rightarrow 422,\ \ 6 \rightarrow 622,\ \ 23 \rightarrow 432.\end{aligned}$$

The dominant role of trigonal P and R $\Sigma1$ twins is apparent. Note that the three twin laws $3(R) \rightarrow 6(P)$, $3(R) \rightarrow 312(P)$ and $32(R) \rightarrow 622(P)$ are $\Sigma3$ obverse/reverse twin laws (*cf.* Table 13 in Klapper & Hahn, 2012).

(vi) Structure determinations of merohedrally twinned crystals are described, with examples and diagrams, in publications by Buerger (1960*a*), Herbst-Irmer & Sheldrick (1998), Herbst-Irmer (2006, Section 7.8.1), Sheldrick (2008), Kahlenberg (1999), Massa (2004), Ferraris (2004) and Klapper & Hahn (2010). Relevant computer programs are listed in Section 3.3.11.6.

3.3.11.4. *Twinning by reticular merohedry (partially-parallel-lattice twins, $\Sigma > 1$ merohedral twins)*

3.3.11.4.1. *General survey*

The $\Sigma3$, $\Sigma5$ and $\Sigma7$ 'twin families', described in the subsequent sections, can be considered as an extension of the $\Sigma1$ merohedral twins, treated in the previous section: instead of the *complete* coincidence of the twin-related lattices, only *partial* coincidence exists, *i.e.* the coincidence lattice is a diluted sublattice of the untwinned crystal lattice. As explained in detail in Sections 3.3.8.2 and 3.3.9.2.3, the sublattice index Σm is the volume ratio of the primitive cells of the twin lattice and the untwinned lattice. Hence $1/m$ is the degree of 'dilution' of the original crystal lattice. In reciprocal space the index Σm is the volume ratio of the primitive cells of the untwinned and the twin lattice, *i.e.* the degree of 'densification' of the reciprocal twin lattice with respect to the reciprocal crystal lattice.

Twins by reticular merohedry, as discussed here, include only Σm twins with 'parallel main axes', which can occur for all lattice parameters and all axial ratios c/a (or rhombohedral angles α) of

[9] Note that point group $\bar{3}2/m$ is a 'lower-symmetry Laue class' for the hexagonal lattice and a 'higher-symmetry Laue class' for the rhombohedral lattice [*cf.* Tables 9(*c*) and (*d*) in Klapper & Hahn, 2010].

a crystal. In these twins all twin elements preserve the orientation of the three-, four- or sixfold main symmetry axis of the lattice. This implies that only twin reflections planes m' parallel and twofold twin axes $2'$ perpendicular to this main axis are possible; for rhombohedral and cubic $\Sigma 3$ twins a plane normal and a twofold twin axis parallel to the (odd!) threefold axis are also possible. Hence, the twinning is always 'two-dimensional', *i.e.* the same reciprocal-lattice layers of the twin partners are superimposed in the reciprocal lattice of the twin.

In contrast to the twins with parallel axes, twins with 'inclined axes' can exist which exhibit coincidences only for special values of the axial ratio c/a or of the rhombohedral angle α. Cases of this type have been derived by Grimmer (1989*a*,*b*, 2003).

In the following, all reciprocal lattices of the Σm twins will be referred to the reciprocal coincidence lattice with basis vectors $\mathbf{a}_m^*$, $\mathbf{b}_m^*$, $\mathbf{c}_m^*$ (*cf.* Figs. 3.3.11.1–6) and not to the lattice of one twin component. This coordinate system has the great advantage that all reciprocal-lattice points of both domain states D(I) and D(II) appear with integral indices HKL.

In the diffraction record of Σm twins, four types of reflections ('coincidence cases') can be distinguished:

(i) reflection HKL is 'doubly coincident', *i.e.* both twin-related D(I) and D(II) reflections are non-extinct and superimposed;

(ii) reflection HKL is present in D(I) and extinct in D(II), *i.e* HKL is a 'single' D(I) reflection;

(iii) reflection HKL is present in D(II) and extinct in D(I), *i.e.* HKL is a 'single' D(II) reflection;

(iv) reflection HKL is 'doubly extinct', *i.e.* absent in D(I) as well as in D(II).

The relative frequencies of these four types as a function of the twin index Σm are presented in Table 3.3.11.1. Noteworthy features are the strong reduction with m of the 'doubly coincident' case (i) and the strong increase of the 'doubly extinct' reflections (iv). The latter case (iv) represents strange 'non-space-group extinctions'. They are an indication of the presence of twinning by reticular merohedry and often a help in determining the twin law [*cf.* Buerger (1960*a*), ch. 5]. The 'single' reflections (ii) and (iii) can be used to determine the volume fractions of the two domain states and, if numerous enough, the crystal structure can even be determined with the stronger of the two sets.

3.3.11.4.2. *The four Σm merohedral twin families*

It is sensible to subdivide the Σm merohedral twins into four families as follows:

Table 3.3.11.1. *Relative frequencies of the four coincidence cases (i)–(iv) for the general Σm twins and the specific twins $\Sigma 3$, $\Sigma 5$ and $\Sigma 7$ treated in this chapter.*

For each twin case the sum of all fractions is 1.

Coincidence cases	Σm	$\Sigma 1$	$\Sigma 3$	$\Sigma 5$	$\Sigma 7$
(i) Coincidence pair	$1/m^2$	1	1/9	1/25	1/49
(ii) Single reflections of domain D(I)	$(m-1)/m^2$	0	2/9	4/25	6/49
(iii) Single reflections of domain D(II)	$(m-1)/m^2$	0	2/9	4/25	6/49
(iv) Doubly extinct reflections	$(m-1)^2/m^2$	0	4/9	16/25	36/49

(i) *The 63 $\Sigma 1$ twins*: complete and exact coincidence of all reflections of the two twin components, treated in Section 3.3.11.3.

(ii) *The 11 rhombohedral and 11 cubic $\Sigma 3$ twins* (obverse/reverse twins, spinel twins) with the four twin laws, represented by (hexagonal/cubic axes)

$$2'[001]/[111], \quad m'(0001)/(111),$$
$$2'[210]/[2\bar{1}\bar{1}], \quad m'(10\bar{1}0)/(2\bar{1}\bar{1});$$

(for the full cosets of these twin laws see Tables 12 and 13 of Klapper & Hahn, 2012). All these twin laws transform an obverse rhombohedron with integral reflection conditions $-h+k+l=3n$ into a reverse rhombohedron with reflection conditions $h-k+l=3n$ and *vice versa*. These four twin laws are different in point groups 3 (rhombohedral) and 23 (cubic), appear in different pairs in point groups $\bar{3}$, 32, $3m$ and $2/m\bar{3}$, 432, $\bar{4}3m$ and form one twin law in groups $\bar{3}2/m$ and $4/m\bar{3}2/m$. These $\Sigma 3$ twins are by far the most frequent among the Σm twins by reticular merohedry. In particular, the cubic spinel twins occur very often in minerals and inorganic compounds.

Illustrations of the direct lattices of the two twin partners and the $l=3n$, $l=3n+1$, $l=3n+2$ layers (hexagonal axes) of the reciprocal twin lattice are given in Figs. 3.3.11.1 and 3.3.11.2. One realizes that for $l=3n$ only doubly coincident and doubly extinct [types (i) and (iv)] but no single reflections [types (ii) and (iii)] occur, whereas for $l=3n+1$ and $l=3n+2$ only single and doubly extinct reflections occur.

Full details, references and examples, particularly of the somewhat complicated cubic $\Sigma 3$ twins, are presented in Sections 3 and 4, Tables 4 and 5, and Appendices A and B of Klapper & Hahn (2012). A survey of structure determinations and refinements of $\Sigma 3$ obverse/reverse twins is provided by Herbst-Irmer (2006) and in Section 3.6 of Klapper & Hahn (2012). Relevant computer programs are listed in Section 3.3.11.6 below.

(iii) *The 12 tetragonal $\Sigma 5$ twins*. Among the tetragonal twins with parallel c axes the smallest possible lattice index is $\Sigma = h^2 +$

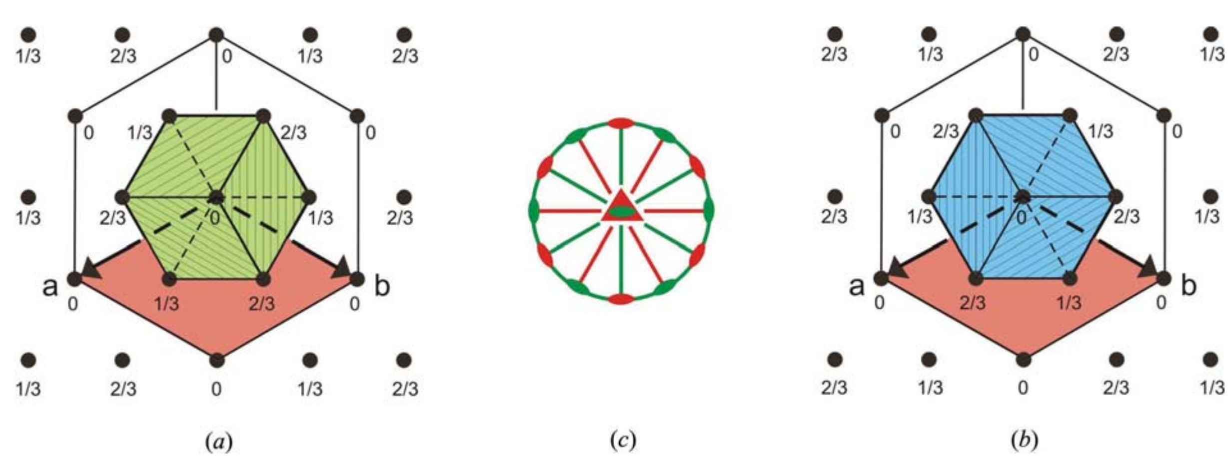

Fig. 3.3.11.1. Rhombohedral $\Sigma 3$ (reverse/obverse) twins in direct space, described with hexagonal axes, viewed down the common c axis. (*a*) Obverse rhombohedral R lattice, with lattice points 0, 0, 0; 2/3, 1/3, 1/3; 1/3, 2/3, 2/3. (*b*) Reverse R lattice, with lattice points 0, 0, 0; 1/3, 2/3, 1/3; 2/3, 1/3, 2/3; dashed lines indicate the lower edges of the primitive rhombohedron. (*c*) Composite symmetry of the twin (stereographic projection), consisting of the *eigensymmetry* elements of the rhombohedron (red) and the set of alternative $\Sigma 3$ twin elements (green); any one of the latter describes the superposition of the two R lattices in the $\Sigma 3$ twin. The coincidence (twin) lattice is a 'diluted' hexagonal P lattice of index 3 and formed by points marked '0' [*cf.* Arnold (2005); this article also contains further diagrams and transformation matrices].

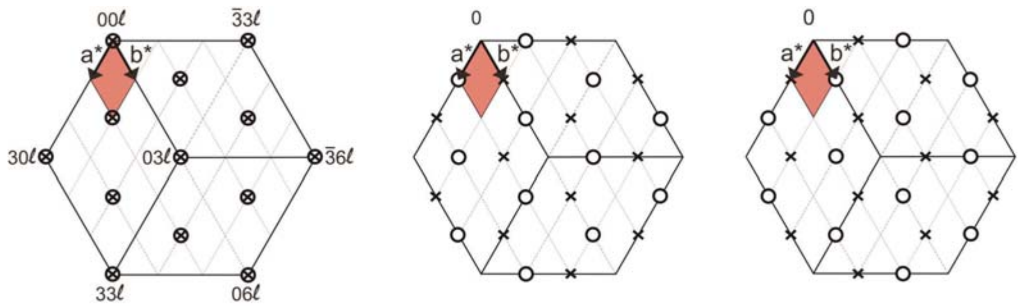

(*a*) $l = 3n$ (*b*) $l = 3n + 1$ (*c*) $l = 3n + 2$

Fig. 3.3.11.2. Reciprocal lattice of the rhombohedral Σ3 twins for the layers $l = 3n$ (*a*), $l = 3n + 1$ (*b*), $l = 3n + 2$ (*c*), described with hexagonal axes. The orientation corresponds to that of the direct lattice in Fig. 3.3.11.1. Circles: obverse twin domain I with reflection condition $-h + k + l = 3n$; crosses: reverse twin domain II with reflection condition $h - k + l = 3n$. In (*a*) all reflections of the two domains coincide; in (*b*) and (*c*) no coincidences, only 'single' reflections occur. In the large cell 00*l*, 30*l*, 33*l*, 03*l* with $l = 0$ and 3, which contains 27 points of the reciprocal twin lattice, three 'doubly coincident' points 000, 110, 220, six 'single' points of domains I and II each, and 12 'doubly extinct' points occur, in accordance with Table 3.3.11.1; the latter are characteristic 'non-space-group' extinctions.

$k^2 = 5$ or $\Sigma = (h^2 + k^2)/2 = 10/2 = 5$ (similarly for $\Sigma = u^2 + v^2$), with twin symmetry (reduced oriented composite symmetry) $4/m\, 2'/m'\, 2'/m'$ and the following twin elements (*cf*. Fig. 3.3.11.3):

$m'(120)$, $m'(2\bar{1}0)$, $2'[120]$, $2'[2\bar{1}0]$ (second position of the twin point-group symbol);

$m'(310)$, $m'(\bar{1}30)$, $2'[310]$, $2'[\bar{1}30]$ (third position of the twin point-group symbol).

In each of the two centrosymmetric tetragonal point groups $4/m$ and $4/m\, 2/m\, 2/m$ these eight elements form one twin law, whereas in the five noncentrosymmetric groups they split in various fashions into two twin laws, resulting in a total of 12 tetragonal Σ5 twin laws (see Table 8 in Klapper & Hahn, 2012).

The *hk*0 plane of the reciprocal lattice of the Σ5 twins is shown in Fig. 3.3.11.4. One recognizes that in the 5 × 5 cell formed by the points 000, 500, 550, 050 (referred to $\mathbf{a}_T$* and $\mathbf{b}_T$*) one doubly coincident reflection 000 (large black circles), four 'single' D(I) (open circles), four 'single' D(II) (crosses) and 16 'doubly extinct' reciprocal lattice points (reflections) occur, thus confirming the entries in Table 3.3.11.1.

Full details of the tetragonal Σ5 twins and their treatment in X-ray diffraction work can be found in Section 5 and Appendix C1 of Klapper & Hahn (2012). Twins of this type are very rare; not more than six structure determinations are known. These are also quoted in the above mentioned paper.

All 12 twin laws of a tetragonal Σ*m* family follow the rule $m = h^2 + k^2 = u^2 + v^2$:

Σ5 with twin elements $m'(120)$ and $2'[120]$,

Σ13 with twin elements $m'(230)$ and $2'[230]$,

Σ17 with twin elements $m'(140)$ and $2'[140]$,

Σ25 with twin elements $m'(340)$ and $2'[340]$ *etc.*

Further Σ*m* values, up to 50, are listed by Grimmer (2003), Table 1. Concrete tetragonal twin cases with Σ*m* higher than 5 are not known.

(iv) *The 14 hexagonal and 26 trigonal Σ7 twins*. The Σ7 twins of the hexagonal crystal family (hexagonal and trigonal crystal

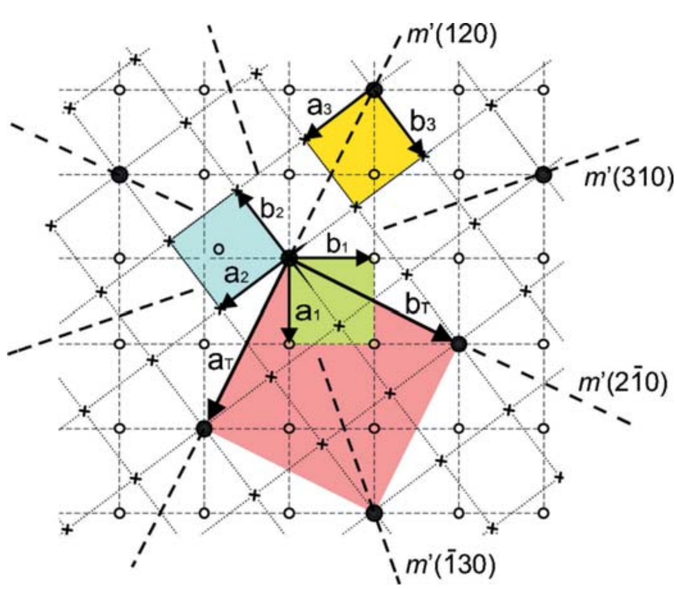

Fig. 3.3.11.3. Tetragonal lattices (**a**–**b** planes, common *c* axis pointing upwards) of twin domain I (start domain, lattice points small circles, right-handed green unit cell $\mathbf{a}_1$, $\mathbf{b}_1$, $\mathbf{c}_1$), of the Σ5 twin-related domain II (small crosses, left-handed blue unit cell $\mathbf{a}_2$, $\mathbf{b}_2$, $\mathbf{c}_2$) and the Σ5 coincidence lattice (large black points, right-handed red unit cell $\mathbf{a}_T$, $\mathbf{b}_T$, $\mathbf{c}_T$). The four alternative twin reflection planes $m'(120)$, $m'(2\bar{1}0)$, $m'(310)$ and $m'(\bar{1}30)$ are indicated by dashed lines. The coordinate axes $\mathbf{a}_2$, $\mathbf{b}_2$, $\mathbf{c}_2$ of domain II (blue) are defined by the reflection plane $m'(120)$. The right-handed yellow unit cell $\mathbf{a}_3$, $\mathbf{b}_3$, $\mathbf{c}_3$ of domain II is obtained from $\mathbf{a}_1$, $\mathbf{b}_1$, $\mathbf{c}_1$ by a clockwise rotation of $\varphi = 2 \arctan (1/2) = 53.13°$ around the tetragonal *c* axis. This cell is commonly used in structure determinations. (From Hahn & Klapper, 2012.)

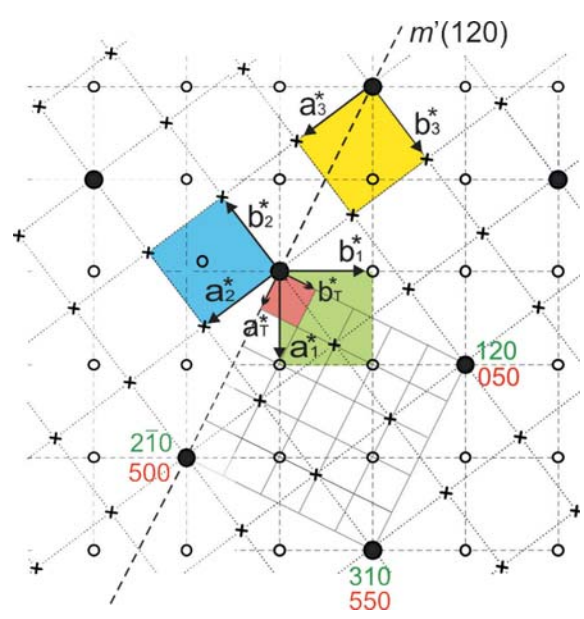

Fig. 3.3.11.4. Reciprocal tetragonal lattices (*hk*0 lattice planes) of twin domain I (start domain, lattice points small circles) and of the Σ5 twin-related domain II (small crosses). The reciprocal lattice of the (direct-space) Σ5 coincidence lattice is represented by the grid of small squares. The unit cells, their handedness and their colours correspond to those of the direct lattices in Fig. 3.3.11.3. In the square formed by the four reciprocal coincidence points 000, $2\bar{1}0$, 310, 120 (in terms of $\mathbf{a}_1$*, $\mathbf{b}_1$*) or 000, 500, 550, 050 (in terms of $\mathbf{a}_T$*, $\mathbf{b}_T$*) there are four 'single' points of twin domains I and II each, one 'coincident' point 000 and, with reference to $\mathbf{a}_T$*, $\mathbf{b}_T$*, 16 'extinct' reciprocal points (*cf.* Table 3.3.11.1). These strange 'non-space-group extinctions' are characteristic of the Σ5 twin law. (From Hahn & Klapper, 2012.)

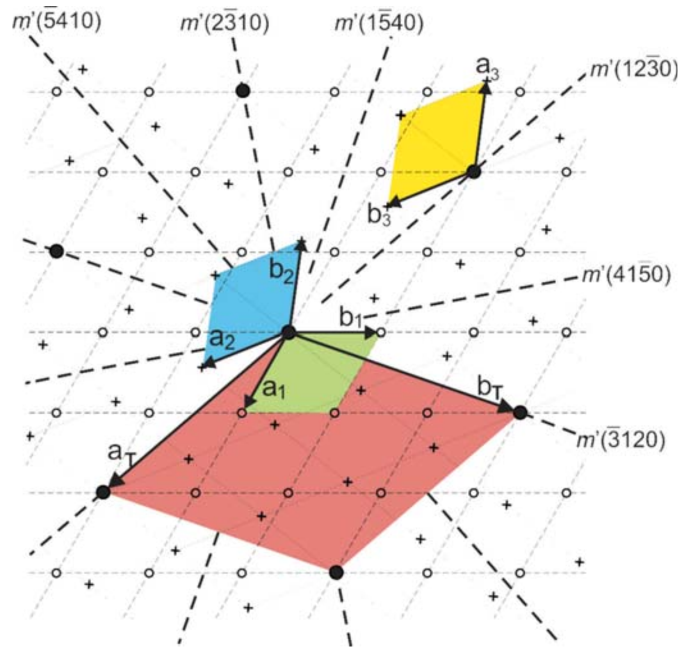

Fig. 3.3.11.5. Hexagonal lattices (**a**–**b** planes, common c axis pointing upwards) of twin domain I (start domain, lattice points small circles, right-handed green unit cell $\mathbf{a}_1$, $\mathbf{b}_1$, $\mathbf{c}_1$), of the $\Sigma7$ twin-related domain II (small crosses, left-handed blue unit cell $\mathbf{a}_2$, $\mathbf{b}_2$, $\mathbf{c}_2$) and of the $\Sigma7$ coincidence lattice (large black points, right-handed red unit cell $\mathbf{a}_T$, $\mathbf{b}_T$, $\mathbf{c}_T$). The six alternative twin reflection planes $m'(12\bar{3}0)$, $m'(\bar{3}120)$, $m'(2\bar{3}10)$, $m'(\bar{5}410)$, $m'(1\bar{5}40)$ and $m'(41\bar{5}0)$ are indicated by dashed lines. The coordinate axes $\mathbf{a}_2$, $\mathbf{b}_2$, $\mathbf{c}_2$ of domain II (blue) are defined by the reflection plane $m'(12\bar{3}0)$. The right-handed yellow unit cell $\mathbf{a}_3$, $\mathbf{b}_3$, $\mathbf{c}_3$ of domain II is obtained from $\mathbf{a}_1$, $\mathbf{b}_1$, $\mathbf{c}_1$ by a clockwise rotation of $\varphi = 120^\circ + 2\arcsin[(1/2)(3/7)^{1/2}] = 120^\circ + 38.2^\circ = 158.2^\circ$ around the hexagonal c axis. This cell is commonly used in structure determinations. (From Hahn & Klapper, 2012.)

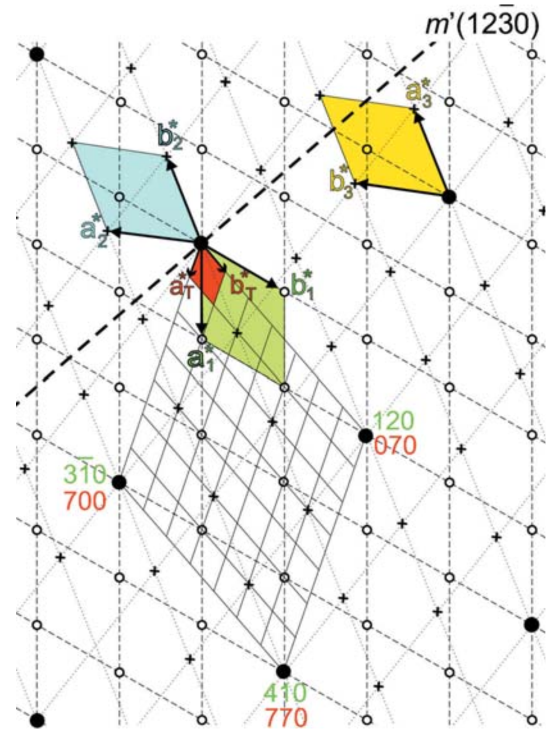

Fig. 3.3.11.6. Reciprocal hexagonal lattices ($hk0$ lattice planes) of twin domain I (start domain, lattice points small circles) and of the $\Sigma7$ twin-related domain II (small crosses). The reciprocal lattice of the (direct-space) $\Sigma7$ coincidence lattice is represented by the grid of small rhombuses. The unit cells, their handedness and their colours correspond to those of the direct lattices in Fig. 3.3.11.5. In the large cell formed by the four reciprocal coincidence points 000, $3\bar{1}0$, 410, 120 (in terms of $\mathbf{a}_1^*$, $\mathbf{b}_1^*$) or 000, 700, 770, 070 (in terms of $\mathbf{a}_T^*$, $\mathbf{b}_T^*$) there are six 'single' points of twin domains I and II each, one 'coincident' point 000 and, with reference to $\mathbf{a}_T^*$, $\mathbf{b}_T^*$, 36 'extinct' reciprocal points (*cf.* Table 3.3.11.1). These strange 'non-space-group extinctions' are characteristic of the $\Sigma7$ twin law. (From Hahn & Klapper, 2012.)

systems, hexagonal P and rhombohedral R lattices) are the hexagonal equivalents of the tetragonal $\Sigma5$ twins treated above. Hence, many features agree: the $\Sigma7$ twins are also parallel c-axes twins, *i.e.* they preserve the hexagonal or trigonal axis and, thus, the twinning is 'two-dimensional' (Fig. 3.3.11.5). Twins with inclined main axes have been derived by Grimmer (1989*a*), but real examples have not yet been observed.

The smallest possible lattice index is $\Sigma = h^2 + hk + k^2 = 7$ or $\Sigma = (h^2 + hk + k^2)/3 = 21/3 = 7$ (similarly for $\Sigma = u^2 - uv + v^2$) for a twin with twin symmetry (reduced oriented composite symmetry) $6/m\,2'/m'\,2'/m'$ and the following four twin laws, represented by:

$m'\{12\bar{3}0\}$, $2'\langle 450\rangle$ (second position of the twin point-group symbol),

$m'\{\bar{5}410\}$, $2'\langle 2\bar{1}0\rangle$ (third position of the twin point-group symbol).

In each of the two *hexagonal* centrosymmetric point groups $6/m$ and $6/m\,2/m\,2/m$ these four twin laws form *one* twin law, whereas in the six noncentrosymmetric point groups (structural settings) they combine in different ways into *two* twin laws.

In the three *trigonal* centrosymmetric point groups (structural settings) $\bar{3}$, $\bar{3}2/m1$ and $\bar{3}12/m$, they combine into two twin laws each, whereas in the remaining five trigonal structural settings all four twin laws are different, leading to 14 hexagonal and 26 trigonal possible $\Sigma7$ twins. Details of these twin cases are presented in Table 10 of Klapper & Hahn (2012).

The reciprocal lattice of the hexagonal $\Sigma7$ twins is shown in Fig. 3.3.11.6. As for the $\Sigma5$ twins, it confirms the data in Table 3.3.11.1: the 7×7 cell formed by the coincident lattice points 000, 700, 770, 070 contains one 'doubly coincident' point 000, six 'single' points of twin domains D(I) and D(II) each and, if referred to $\mathbf{a}_T^*$ and $\mathbf{b}_T^*$, 36 'doubly extinct' points.

Section 6 and Appendix C2 of the paper by Klapper & Hahn (2012) contains full details of the hexagonal $\Sigma7$ twins and their treatment in diffraction and structure work. Twins of this kind have not been found so far. This also applies to the $\Sigma7$ twins of crystals with a rhombohedral R lattice [the frequent rhombohedral $\Sigma3$ twins are treated above under (ii)]. Their (somewhat complicated) twin phenomena are also described in the above-mentioned paper.

Beyond the 'starting type' $\Sigma7$, the following twins also belong to this family:

$\Sigma13$ with $m'\{31\bar{4}0\}$ or $2'\langle 140\rangle$ (second position of the point-group symbol),

$\Sigma19$ with $m'\{32\bar{5}0\}$ or $2'\langle 250\rangle$ (second position of the point-group symbol), similarly for higher Σ values.

Twins of this hexagonal/trigonal Σm 'family' are not known.

3.3.11.5. *Pseudo-merohedral twins*

3.3.11.5.1. *General remarks*

This type of twins includes both pseudo-merohedral $\Sigma1$ and $\Sigma m > 1$ twins. It refers to small deviations from strict full or partial lattice coincidence of the twin partners. Pseudo-merohedral twins occur if metrical (but not necessary structural) pseudosymmetries occur in a crystal and, hence, the twin element belongs to the symmetry of a higher crystal system. Frequently occurring typical examples are monoclinic crystals with the angle β very close to 90° (simulating an orthorhombic crystal) or with approximately $a = c$ (simulating a B-centred orthorhombic crystal), orthorhombic crystals with nearly $b/a \simeq \sqrt{3}$ (simulating a hexagonal crystal, *cf.* examples below), or a tetragonal crystal with $c/a \simeq 1$ (simulating a cubic crystal). In contrast to twins by strict $\Sigma1$ merohedry the twin operation is *not* a symmetry operation of the holohedry of the untwinned crystal. Thus the

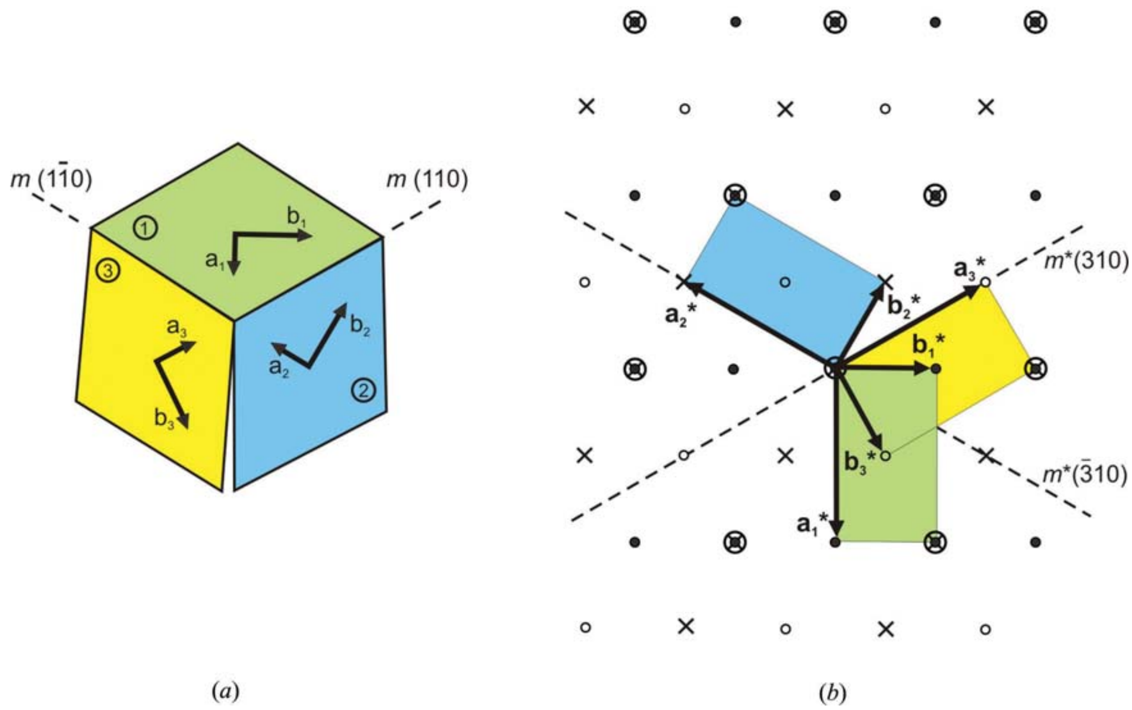

Fig. 3.3.11.7. (*a*) Morphologically idealized pseudo-hexagonal threefold sector twin of an orthorhombic crystal with b/a = tan 58.5°, generated by the two symmetry-equivalent twin mirror planes (110) and (1$\bar{1}$0). In real growth twins the gap (here about 5°) is closed with an irregular twin boundary (*cf.* Fig. 3.3.2.4). For b/a > tan 60° there is a (formal) overlap of domains 2 and 3. (*b*) Reciprocal-lattice plane *hkl* (l = 0, 1, 2, ...) of the threefold pseudo-hexagonal twin shown in (*a*), viewed along the pseudo-hexagonal c^* axis, but drawn with exactly b/a = tan 60°. It shows the superposition of the three lattices of domain 1 (black dots), domain 2 (crosses) and domain 3 (open circles). Lattice points with $h + k = 2N$ are threefold coincident, the others are single. This holds for all layers $l = 0, \pm1, \pm2, \ldots$. Note that the twin reflection planes $m'(110)$ and $m'(1\bar{1}0)$ in direct space correspond to the planes $m^*(310)$ and $m^*(\bar{3}10)$ in reciprocal space, respectively.

twin-related reciprocal-lattice points (reflections) are *not symmetry equivalent* and have *different* structure-factor moduli (diffraction case B1). Exceptions are those few reflections which are mapped by the twin operation upon themselves or their opposites.

Twins of this type in direct space, with many examples, have been discussed already in Sections 3.3.8.4 and 3.3.8.5, introducing the terms 'twin obliquity' ω and lattice index $[j]$ as given by Friedel (1926). Further treatments are contained in Sections 3.3.9.2 and 3.3.9.3. The number of possible pseudo-merohedral twin laws is very great (much larger than the 'strict' merohedral $\Sigma1$ and $\Sigma > 1$ twin laws) and, hence, only examples and general rules for the experimental work can be given here.

In reciprocal space, three border cases of pseudo-merohedral twins are important:

(i) The splitting of the reflections in the entire accessible twin diffraction record is so small that they appear as 'untwinned' or, at least, as unresolvable reflections, possibly with wrong unit cell and symmetry. In these cases very often twinning will not even be recognized and, as a result, the structure determination may fail. Even if the twinning is suspected as 'strictly merohedral', the structure determination may fail or present severe problems because the twin law is of a non-merohedral and difficult type.

(ii) The opposite case is a diffraction record in which many reflections (those with higher 2θ values) are clearly split, even if reflections with small 2θ values are not resolved. The resolved pairs of reflections can then be used to determine the twin law, but not the volume fraction of the twin because their F moduli are different. With the intensity data of the stronger reflection set (*i.e.* of the larger twin partner), however, the structure can often be solved, as described in Section 3.3.11.2.

(iii) A problem is also provided by twins in which all (or nearly all) reflections of the diffraction record overlap, but are not fully 'split'. Here, twinning is usually recognizable but the main problem is the separation of the many overlapped unresolved reflections in order to arrive at the two 'true' sets of intensities with which a successful structure determination can be performed. There are several computer programs which are designed to split overlapped reflections, quoted in Section 3.3.11.6, but in many cases in addition intuition by the researcher and examination of several twinned crystals, with different volume fractions, is required.

3.3.11.5.2. *Example: pseudohexagonal (cyclic) twins of orthorhombic crystals (pseudo-coincident* $\Sigma3$ *twins)*

This kind of twinning with $m'(110)$ and $m'(1\bar{1}0)$ or pseudo-threefold twin axis is often observed in orthorhombic crystals with nearly ortho-hexagonal metric, *i.e.* with an axial ratio $b/a \simeq \sqrt{3}$ = tan 60° (pseudo-hexagonal axis c). Prominent examples are aragonite (Fig. 3.3.2.4; b/a = tan 58.1°), K_2SO_4 (Fig. 3.3.6.9; b/a = tan 60.18°), NH_4LiSO_4 (Fig. 3.3.7.2; b/a = tan 59.99°) and $(NH_4)_2SO_4$ (b/a = tan 60.85°), all having a primitive (not a C-centred, see below) lattice. They often appear as 'growth-sector twins' with three sector domains (Figs. 3.3.2.4 and 3.3.7.2*a*), six sector domains (Fig. 3.3.6.9 with equal orientation of opposite sectors) or with a more-or-less irregular distribution of the sectors (Fig. 3.3.7.2*b*). A morphologically idealized triple-sector twin is shown in Fig. 3.3.11.7(*a*). Apart from the reflection intensities, the diffraction patterns of these triple twins, showing a pseudo-hexagonal arrangement of diffraction spots, are independent of the size, shape and distribution of the sector domains. Sometimes twins with only two domain orientations, related by $m'(110)$ or $m'(1\bar{1}0)$, occur.

(i) *Pseudo-hexagonal (cyclic) twins based on an orthorhombic* P *lattice*. For an easier understanding of the superposition and coincidence behaviour of twin-related reflections of the domains 1, 2 and 3 shown in Fig. 3.3.11.7(*a*), the basis vectors $\mathbf{a}_2$, $\mathbf{b}_2$, $\mathbf{c}_2$ and $\mathbf{a}_3$, $\mathbf{b}_3$, $\mathbf{c}_3$ are generated from the basis vectors $\mathbf{a}_1$, $\mathbf{b}_1$, $\mathbf{c}_1$ of start domain 1 for *exact hexagonal metric*, as follows:

$$\mathbf{a}_2 = -\tfrac{1}{2}(\mathbf{a}_1 + \mathbf{b}_1), \quad \mathbf{b}_2 = \tfrac{1}{2}(-3\mathbf{a}_1 + \mathbf{b}_1), \quad \mathbf{c}_2 = \mathbf{c}_1, \qquad (1)$$

$$\mathbf{a}_3 = \tfrac{1}{2}(-\mathbf{a}_1 + \mathbf{b}_1), \quad \mathbf{b}_3 = \tfrac{1}{2}(3\mathbf{a}_1 + \mathbf{b}_1), \quad \mathbf{c}_3 = \mathbf{c}_1. \qquad (2)$$

Correspondingly for Miller indices:

$$h_2 = -\tfrac{1}{2}(h_1 + k_1), \quad k_2 = \tfrac{1}{2}(-3h_1 + k_1), \quad l_2 = l_1, \qquad (3)$$

$$h_3 = \tfrac{1}{2}(-h_1 + k_1), \quad k_3 = \tfrac{1}{2}(3h_1 + k_1), \quad l_3 = l_1. \qquad (4)$$

For a *pseudo-hexagonal metric* the coefficients of the transformation matrices deviate more or less from their ideal values $\pm 1/2$ and $\pm 3/2$. It is easily recognized that coincidence of reflections is obtained only if all indices $h_2k_2l_2$ and $h_3k_3l_3$ are integer, *i.e.* if the condition $h_1 + k_1 = 2N$ (and correspondingly $h_2 + k_2 = 2N$ and $h_3 + k_3 = 2N$) is fulfilled. Thus, for pseudo-hexagonal twins with a primitive lattice (no lattice extinctions) and parallel c axes, two sets of reflections are distinguished:

(*a*) Reflections hkl with $h + k = 2N$: for exact hexagonal metric with $b/a = \sqrt{3} = \tan 60^\circ$ these reflections of all domains coincide exactly, as shown in Fig. 3.3.11.7(*b*). For a pseudo-hexagonal metric these reflections are, depending on the deviation from exact hexagonality, more-or-less split into three spots (for three domains states) or two spots (for two domain states).

(*b*) Reflections hkl with $h + k = 2N + 1$: these are 'single' for each domain state, forming an exact hexagonal twin diffraction pattern for $b/a = \sqrt{3}$ and a more-or-less distorted hexagonal pattern for $b/a \neq \sqrt{3}$.

The occurrence of both single and (pseudo-)coincident reflections in the diffraction pattern classifies the pseudo-hexagonal twins of orthorhombic crystals with a P lattice as twins by reticular pseudo-merohedry of index 2. Note that the entire diffraction record is pseudo-hexagonal without any 'non-space-group' extinctions (*cf.* Section 3.3.11.4.1).

(ii) *Special reflection sets, their coincidences and diffraction cases for pseudo-hexagonal orthorhombic centrosymmetry.* Since the twin elements $m'(110)$ and $m'(1\bar{1}0)$ *do not belong to the eigensymmetry* of the untwinned crystal, the twin-related reflections (of domains 1 + 2, 1 + 3, as well as 2 + 3) are in general not symmetry-equivalent and have different F moduli (diffraction cases B1). There are, however, two special types of reflections which are equivalent and coincident or pseudo-coincident and have equal F moduli (diffraction cases A):

(*a*) Twin-related reflection pairs $(hhl)_1/(\bar{h}\bar{h}l)_2$ (twin element $m'(110)$, equation (3) above, common zone axis $[1\bar{1}0]$) and $(h\bar{h}l)_1/(\bar{h}hl)_3$ (twin element $m'(1\bar{1}0)$, equation (4) above, common zone axis [110]): The reflections of each of these pairs coincide exactly (for any b/a ratio) and have equal F moduli. The twin-related reflections of the third domain, $(0{,}2h{,}l)_3$ for $m'(110)$ and $(0{,}\overline{2h}{,}l)_2$ for $m'(1\bar{1}0)$, are more-or-less separated from the coincident reflections of the pairs $(hhl)_1/(\bar{h}\bar{h}l)_2$ and $(h\bar{h}l)_1/(\bar{h}hl)_3$ and have different F moduli. This is also the case for $(hh0)_1$ and $(h\bar{h}0)_1$, *i.e.* the reflecting planes parallel to the twin mirror planes. Furthermore, for reflections $00l$, the diffraction spots of *all three* domains *coincide* and have *equal F* moduli. Thus, if both $m'(110)$ and $m'(1\bar{1}0)$ are active and form a triple twin, the triple diffraction spot consists of reflections of type hhl, $\bar{h}\bar{h}l$ (coincident, equal F moduli) and $0{,}2h{,}l$ (split, different F modulus).

(*b*) Twin-related pairs $(h{,}\overline{3h}{,}l)_1/(h{,}\overline{3h}{,}l)_2$ [twin element $m'(110)$, equation (3) above, slightly different zone axes [310] pseudo-perpendicular to the twin plane] and $(h{,}3h{,}l)_1/(h{,}3h{,}l)_3$ [$m'(1\bar{1}0)$, equation (4) above, slightly different zone axes $[3\bar{1}0]$ pseudo-perpendicular to the twin plane]: The twin-related reflections of these pairs are split but have equal F moduli (diffraction case A).[10] The twin-related reflection of the third domain is $(\overline{2h}0l)_3$ for $m'(110)$ and $(\overline{2h}0l)_2$ for $m'(1\bar{1}0)$. Thus, if both $m'(110)$ and $m'(1\bar{1}0)$ are active and form a triple twin, the triple diffraction spot consists of three split reflections of type $h{,}\overline{3h}{,}l$, $h{,}3h{,}l$ and $\overline{2h}{,}0{,}l$, the former two having equal F moduli.

[10] This can be illustrated by the interpretation of reflection sets $\{hkl\}$ as face forms (crystal forms) $\{hkl\}$ and their *eigensymmetries*, as described in two papers by Klapper & Hahn (2010, 2012).

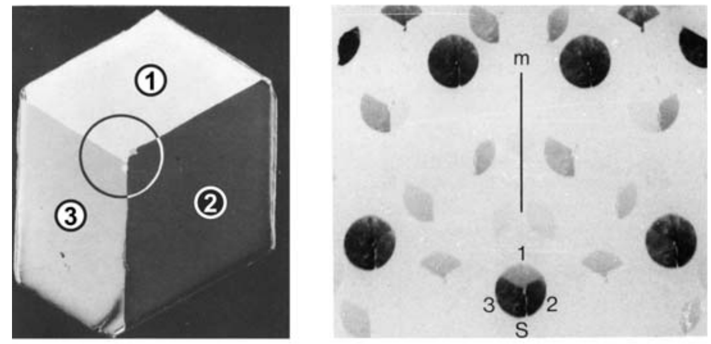

(*a*) (*b*)

Fig. 3.3.11.8. (*a*) (001) plate of ammonium lithium sulfate, NH_4LiSO_4, (about 11 mm diameter, 0.8 mm thick) between crossed polarizers, exhibiting sectorial pseudo-hexagonal growth twinning. The circle around the triple point of the three domains marks the area intercepted by the white synchroton beam for recording a topographic Laue pattern. (*b*) Part of the topographic Laue pattern taken with white-beam synchrotron radiation (SRS Daresbury) along the pseudo-hexagonal axis from the encircled region of the twin shown in (*a*). (For the whole Laue pattern see Fig. 4 of Docherty *et al.*, 1988). The Laue spots appear as small topographs of the 120° twin sectors hit by the white beam. For reflections with $h + k = 2N$ the three sectors are simultaneously imaged; for all other reflections ($h + k = 2N + 1$) only single sectors appear. The affiliation to the three domains is recognized from the orientation of their 120° sectors. Owing to the very small metrical deviation $b/a = \tan 59.95^\circ$ from exact hexagonality (gap angle 0.15°) there is practically no splitting of the coincident reflections, *i.e.* no mutual tilt of their lattice planes and, thus, no separation or partial overlapping of their topographic images. Note the vertical mirror plane m. In the triple Laue spot S the reflection types described in Section 3.3.11.5.2 paragraph (*b*) are present, *i.e.* two reflections of type $h{,}3h{,}l$ imaging domains 2 and 3 (symmetry-equivalent, equal F moduli) and reflection of type $2h{,}0{,}l$, imaging domain 1 (different F modulus).

This case is presented by the Laue-diffraction spot S in Fig. 3.3.11.8(*b*).

The superposition of the reciprocal P lattices of the three twin domains, corresponding to those shown in Fig. 3.3.11.7(*a*), however with exact $b/a = \tan 60^\circ$, is presented in Fig. 3.3.11.7(*b*). It shows single ($h + k = 2N + 1$) and triply coincident ($h + k = 2N$) lattice points, as derived by the above transformations. Figs. 3.3.11.8(*a,b*) present an illustration of the diffraction and coincidence features of triply pseudo-hexagonal growth-twinned orthorhombic NH_4LiSO_4 (point group $2mm$, gap angle $\simeq 0.1^\circ$). It shows a section of an X-ray topographic Laue pattern of the circular region centred on the meeting point of the domains [shown in Fig. 3.3.11.7(*a*); splitting of the reflections is practically zero]. A similar topographic Laue pattern of a ferroelastically introduced twin (100) lamellae embedded in a (001) plate of pseudo-hexagonal $(NH_4)_2SO_4$ (point group mmm, overlap angle 5°, very strong splitting) is presented by Docherty *et al.* (1988). In this case, the Laue diffraction pattern does not show any symmetry, due to the presence of only two non-symmetrically arranged domain states.

An illustrative description of the diffraction patterns of pseudo-hexagonal twins of crystals with a primitive orthorhombic P lattice and its application to the X-ray topographic study of twins and their boundaries in NH_4LiSO_4 is given by Klapper (1987, pp. 372–378). Another study of pseudo-hexagonal twinning of NH_4LiSO_4 and $(NH_4)_2SO_4$, using synchroton Laue topography, is presented by Docherty *et al.* (1988).

(iii) *Pseudo-hexagonal twins of orthorhombic crystals based on a C lattice*. In the orthorhombic C lattice, reflections of all domains with $h + k = 2N + 1$ are extinct, and therefore single reflections do not occur in the superposition of the diffraction patterns of the three domains. Only triply (pseudo-)coincident reflections with $h + k = 2N$ occur. This is an example of a $\Sigma 1$ *twinning by pseudo-merohedry*. All other diffraction features are the same as those quoted above for twins of orthorhombic crystals with a P lattice.

(iv) *Additional remark*. The pseudo-hexagonal triple growth twins are morphologically often described by a pseudo-threefold rotation with angle $\phi' = 2\arctan(b/a)$, clockwise ($\phi'+$) for domain pair $1 \rightarrow 2$ and anticlockwise ($\phi'-$) for domain pair $1 \rightarrow 3$, both together approximately filling the full 360° circle. The basis-vector transformations (1) and (2) given above for $m'(110)$ and $m'(1\bar{1}0)$ have to be modified as follows: The vectors $\mathbf{a}_2$ and $\mathbf{a}_3$ remain unchanged, whereas $\mathbf{b}_2$ and $\mathbf{b}_3$ are inverted into their opposites $-\mathbf{b}_2$ and $-\mathbf{b}_3$, thus leading to right-handed coordinate systems for domains 2 and 3. Similarly for h_2, k_2, h_3 and k_3 [equations (3) and (4) above]. Since the reversal of the axis $\mathbf{b}$ is part of the *eigensymmetry* of point group *mmm*, the effect of $\phi'+$ and $\phi'-$ is the same as that of $m'(110)$ and $m'(1\bar{1}0)$. Thus each of the three twin elements $m'(110)$, $2'_{\rm irrat} \simeq [310]$ and $\phi'+$ represents in point group *mmm* the same orientation relation for domain pair $1 \rightarrow 2$. Similarly: $m'(1\bar{1}0)$, $2'_{\rm irrat} \simeq [3\bar{1}0]$ and $\phi'-$ for domain pair $1 \rightarrow 3$.

For the hemihedral point groups 222 and *mm*2, *m*2*m*, 2*mm* these results have to be modified. For group 222 the two reflection twin elements lead to opposite handedness of domains 1 and 2 and 1 and 3, but equal handedness of domains 2 and 3, whereas twin elements $2'_{\rm irrat}$ and $\phi'\pm$ provide equal handedness of all three domains. For point group *mm*2 *etc.* the situation is more complicated due to the different settings with the polar axis along **a**, **b** or **c**, which physically lead to polar domains with different head-to-tail, head-to-head and tail-to-tail domain boundaries. These cases are not further analysed here.

Concerning the diffraction patterns of pseudo-hexagonal twins of hemihedral orthorhombic crystals: The splitting of diffraction spots is a matter of the lattice metric and independent of the point group. Regarding reflection intensities: among the triply split reflections only reflections of sets $\{hhl\}$ and $\{h,3h,l\}$ may undergo a change from diffraction case A in point groups *mmm* to diffraction case B2 in the hemihedral groups.

3.3.11.6. *Programs for structure determinations with twinned crystals*

Programs for the determination of crystal structures from merohedral and pseudo-merohedral twins are, among others, *SFLS* (Eitel & Bärnighausen, 1986), *TWINXLI* (Hahn & Massa, 1997), *TWIN* 3.0 (Kahlenberg & Messner, 2001), *CRYSTALS* 12 (Betteridge *et al.*, 2003), *JANA*2006 (Petricek *et al.*, 2006), *DIRAX* (A. J. M. Van Duisenberg, University of Utrecht, The Netherlands; e-mail: duisenberg@chem.uu.nl) and especially *SHELXL* (Sheldrick, 1997).

Detailed descriptions of the (widely used) *SHELXL* program system for structure determinations and for refinements of merohedrally and pseudo-merohedrally twinned crystals are provided by Herbst-Irmer & Sheldrick (1998, 2002), by Guzei *et al.* (2012) and, in particular, by Herbst-Irmer (2006).

Textbook descriptions of structure determinations of twins are provided by Buerger (1960*a*), Massa (2004) and Ferraris (2004). Systematic analyses of the diffraction intensities of all Σ1, Σ3, Σ5 and Σ7 merohedral twins are contained in two publications by Klapper & Hahn (2010, 2012).

The following note on domain structures is supplied by V. Janovec. It describes briefly and clearly how strategies used in the study of 'domain structures', treated in Chapter 3.4, can be used for the investigation of twins. Section 3.3.12 thus forms a bridge between the present chapter on *Twinning* and the following chapter on *Domain structures*.

3.3.12. Domain structures (by V. Janovec)

Domain structure is a special kind of twinning which *results from lowering of crystal symmetry* at a phase transition. A homogeneous phase with higher symmetry (called the *parent phase*) breaks into a non-homogeneous twinned phase (ferroic phase) with lower symmetry in which the twin partners (*domains*) are related by twinning operations that are crystallographic operations disappearing at the transition (for different terminology used in twinning and domain structures, see Table 3.4.2.4).

Domains have lower symmetry than the parent phase. As a result, domains acquire additional physical properties called *spontaneous properties*. When observed by certain apparatus (*e.g.* a microscope), anisotropic domains exhibit different properties and thus can be observed and identified in direct space. This distinction of domains in direct space by means of their spontaneous properties thus provides important additional information to the examination of twinning of the material by diffraction methods.

It turns out that symmetry lowering at the transition exactly determines which spontaneous quantities are distinct in the two different domains of a domain twin. Unfortunately, this useful consideration cannot be performed with twins which originate from means other than a phase transition, *e.g.* growth twins. It is, however, possible to check whether the nonexistent high-symmetry parent phase can be substituted by a so-called *composite symmetry* of the twin, even though a phase of the crystal with this symmetry does not exist in reality. This means that we *treat a twin as a domain twin resulting from a nonexistent (hypothetical) phase transition*.

This is why it is expedient to have at one's disposal tables of possible phase transitions from all possible composite symmetries. These tables can be found in Sections 3.4.3 and 3.4.4 of Chapter 3.4. Several examples show how these tables can be utilized in twin analysis.

3.3.13. Glossary

(hkl)	crystal face, lattice plane, net plane (Miller indices)
$\{hkl\}$	crystal form, set of symmetry-equivalent lattice (net) planes
$[uvw]$	zone axis, crystal edge, lattice direction, lattice row (direction indices)
$\langle uvw\rangle$	set of symmetry-equivalent lattice directions (rows)
$\mathcal{G}$	symmetry group of the (real or hypothetical) 'parent structure' or high-symmetry modification or 'prototype phase' of a crystal; group in general
$\mathcal{H}$	*eigensymmetry* group of an (untwinned) crystal; symmetry group of the deformed ('daughter') phase of a crystal; subgroup
$\mathcal{H}_1, \mathcal{H}_2, \ldots, \mathcal{H}_j$	oriented *eigensymmetries* of domain states $1, 2, \ldots, j$
$\mathcal{H}^*_{1,2}$, $\mathcal{H}^*$	intersection symmetry group of the pair of oriented *eigensymmetries* $\mathcal{H}_1$ and $\mathcal{H}_2$, reduced *eigensymmetry* of a domain
$\mathcal{K}$	composite symmetry group of a twinned crystal (domain pair); twin symmetry
$\mathcal{K}^*_{1,2}$, $\mathcal{K}^*$	reduced composite symmetry of the domain pair (1, 2)
$\mathcal{K}(n)$	extended composite symmetry of a twinned crystal with a pseudo n-fold twin axis
$k, k_1, k_2, \ldots, k_i$	twin operations (k_1 = identity)
$2'$, m', $\bar{1}'$, $\bar{4}'(2)$, $6'(3)$, $\bar{3}'(3)$, $\bar{6}'(3)$	twin operations of order two in colour-changing (black–white) symmetry notation
$\lvert\mathcal{G}\rvert$, $\lvert\mathcal{H}\rvert$, $\lvert\mathcal{K}\rvert$	order of group $\mathcal{G}$, $\mathcal{H}$, $\mathcal{K}$
$[i]$	index of $\mathcal{H}$ in $\mathcal{G}$, or of $\mathcal{H}$ in $\mathcal{K}$
$[j]$, Σ	index of coincidence-site lattice (twin lattice, sublattice) with respect to crystal lattice